Quantifying greenspace with satellite images in Karachi, Pakistan using a new data augmentation paradigm

Miao Zhang[1], Hajra Arshad[2], Manzar Abbas[2], Hamzah Jehanzeb[2], Izza Tahir[2], Javerya Hassan[2], Zainab Samad[2,3], Rumi Chunara[1,4,*]

[1]New York University, Department of Computer Science and Engineering, New York, USA
[2]Aga Khan University, Department of Medicine, Karachi, Pakistan
[3]Aga Khan University, Department of Medicine, CITRIC Health Data Science Center, Karachi, Pakistan
[4]New York University, Department of Biostatistics, New York, USA
*Corresponding author: Rumi Chunara (rumi.chunara@nyu.edu)

Abstract

Greenspaces in communities are critical for mitigating effects of climate change and have important impacts on health. Today, the availability of satellite imagery data combined with deep learning methods allows for automated greenspace analysis at high resolution. We propose a novel green color augmentation for deep learning model training to better detect and delineate types of greenspace (trees, grass) with satellite imagery. Our method outperforms gold standard methods, which use vegetation indices, by 33.1% (accuracy) and 77.7% (intersection-over-union; IoU). The proposed augmentation technique also shows improvement over state-of-the-art deep learning-based methods by 13.4% (IoU) and 3.11% (accuracy) for greenspace segmentation. We apply the method to high-resolution (0.27 m/pixel) satellite images covering Karachi, Pakistan and illuminates an important need; Karachi has 4.17 m^2 of greenspace per capita, which significantly lags World Health Organization recommendations. Moreover, greenspaces in Karachi are often in areas of economic development (Pearson's correlation coefficient shows a 0.352 correlation between greenspaces and roads, $p < 0.001$), and corresponds to higher land surface temperature in localized areas. Our greenspace analysis and how it relates to infrastructure and climate is relevant to urban planners, public health and government professionals, and ultimately the public, for improved allocation and development of greenspaces.

This manuscript is an EarthArXiv preprint and will be submitted for possible publication in a peer-reviewed journal. Subsequent versions of this manuscript may have slightly different content. Please feel free to contact the corresponding author for

feedback.

1 Introduction

"Greenspaces" are defined by the U.S. Green Building Council as land that is partly or completely covered with trees, shrubs, grass, or other vegetation. There is a large amount of literature highlighting the environmental, sociocultural, and economic benefits of greenspaces. Briefly, these facilities can be used as therapeutic spaces for rehabilitation exercises, thereby improving the health of its residents, play an important role in biodiversity conservation, contributes to aesthetics, increase economic value, provide nature-based solutions for resiliency (e.g., rainwater management, sewage overflow and flood control), reduce the heat island effect by providing shade and lowering surface temperatures, and also serve as a place to relax and strengthen social organization [60, 27, 54, 30, 12, 48].

Recently, shrinkage of greenspaces due to population growth, industrial expansion, developmental activities, and land encroachment has led to disruption of the ecological balance in many urban centers including in Pakistan [67]. This change is particularly important due to the crucial role of greenspaces for climate change mitigation via several mechanisms; carbon sequestration (greenspaces act as carbon sinks by absorbing and storing carbon dioxide from the atmosphere), reduced energy consumption (greenspaces provide shade and reduce the urban heat island effect, which helps decrease energy consumption for cooling buildings), stormwater management (greenspaces absorb and filter rainwater, reducing the load on stormwater infrastructure and preventing water pollution), air quality improvement (greenspaces improve air quality), biodiversity conservation (greenspaces provide habitats for diverse species and diversifying ecosystems enhance resilience and capacity to adapt to climate change impacts). In sum, greenspaces positively affect quality of life across both physical and mental health, and provide various ecological, socio-cultural, and economic benefits to a community. Thus, it is essential to strategically measure and inform urban planning and public health interventions with significant consideration for greenspaces, to develop a sustainable future [83, 39].

New analytic methods and data sources illuminate the opportunity for measuring greenspaces in countries which the environmental, sociocultural, and economic benefits have not been quantified. An important exemplar is Karachi, one of the largest cities in the world in terms of urban population. Karachi also has a high urban population density of over 24,000 people/km^2, which far surpasses that of other megacities such as Beijing or New York City [94]. These challenges place greater pressure on limited greenspaces, making their preservation and accessibility crucial for providing recreational opportunities and improving the quality of life for the densely populated areas. Another important reason to focus on Karachi is the current lack of knowledge on greenspaces in Pakistan; studies to-date have been focused on specific geographic areas (e.g. cemeteries in Lahore [67]) or study greenspace largely via survey data [72, 81].

Satellite imagery is an important data source that has been utilised to measure greenspace for decades. Specifically, several vegetation indices have been derived using spectral bands and their ratios [86, 57, 34, 58, 11]. New opportunities for imagery include new satellites offering higher resolution (0.5 m/pixel or less). Beyond measurement of greenspaces, it is also important to distinguish types of greenspaces in order to identify the quantity of each type and inform work improving types that bring the greatest benefits to citizens. Though challenging to obtain via standard greenspace cataloging (manual data gathering or vegetation indices), such detailed knowledge would enable urban planners to augment and repurpose greenspaces strategically.

Researchers have proposed leveraging deep learning along with satellite imagery (examples of such shown in Fig. 1) to detect vegetation land cover [39, 56, 5, 52, 23, 88] and to classify vegetation types [61, 6, 101], via the algorithm of semantic segmentation. Studies have largely focused on examining landscapes in specific local sites with few exceptions (greenspace has been catalogued using deep learning, for four cities in China [56, 21] and the country of Slovenia [6]; but the resolution of the satellite images used is low (1-10 m/pixel). Moreover, compared to prior work, a unique challenge approached in this work is the limited amount of greenspace in Karachi; The training data includes only 30.3% of pixels labelled with any types of greenspace, and further, the grass class label only takes 11.3% of total pixels. This problem of class scarcity hinders deep neural network training, which relies on large volumes of data to extract representative landscape features [80, 105]. Though studies have adopted image augmentation techniques including random flips, rotations, brightness and contrast change to tackle class scarcity [42, 17, 91], such techniques only increase data variety with respect to basic image properties, and do not provide additional information for the important target feature, greenspace. Therefore, we propose to design augmentation for model to learn wide range of features for diverse greenspace landscapes.

Our contribution is three-fold:

1. We provide a new high resolution satellite image dataset for semantic segmentation (2480 images of 512×512 pixels), with pixel-level greenspace class annotations[1]. The data is expected to facilitate future satellite image analysis research and contribute to its geographic diversity.

2. We propose a simple but effective augmentation strategy by shifting the green hue of images to improve model recognition robustness for greenspace variations. Experimental results demonstrate improvements over state-of-the-art methods by a substantial margin.

3. We apply our method to quantify greenspace over all 173 union councils in Karachi, Pakistan and demonstrate their associations to economic development reflected by paved road construction, and urban heat by land surface temperature (LST). Given the global importance of greenspaces for improved planetary and human health, our method is relevant to, and can be extended to locations worldwide.

2 Related work

2.1 Land cover recognition with satellite imagery

Land use and land cover have been recognized with satellite images which document Earth surface. Studies characterize multiple land uses such as water body, forest, build-up area, and their changes from Landsat satellite images. The results have shown utility for indicating urbanization [98, 20, 2] and surface temperature [20, 47]. By combining spectral bands of satellite images, different indices have been used to analyze land cover objects. For example, the normalized difference water index (NDWI) uses green and near infra-red bands for water bodies [32, 96], the normalized difference built-up index uses red and blue bands [104] to map built-up areas (e.g., urban residential, commercial or industrial areas). Vegetation indices to

[1]Image data source and annotations can be accessed at https://github.com/ChunaraLab/GreenSpaceAnalysis.

detect green biomass include normalized difference vegetation index (NDVI) [100] which uses visible bands of wavelength 620-670 nm and infrared bands of wavelength 841-8756 nm, green-red vegetation index (GRVI) [62] which uses visible bands of wavelength 545-565 nm and 620-670 nm, chlorophyll/carotenoid index (CCI) [31] which uses visible bands of wavelength 526-536 nm and 620-670 nm, etc.

In more recent years, deep learning as a class of machine learning methods has demonstrated its superiority in multiple land cover recognition tasks. This approach is used to extract landscape features by multi-layer processing and generate prediction rules from labeled image data. Specifically, semantic segmentation algorithms are used to predict land cover object outlines by pixel-level classification [102]. The algorithms are learnt with encoder-decoder model architectures, including UNet [74], PSPNet [107], DeepLabV3+ [18], SAM [50], etc. Since deep learning methods do not require hand-crafted features or indices, they are easily adapted to new recognition tasks such as generating closed field boundary [89], road detection with occlusions of trees and cars [22], cloud and cloud shadow detection [14], etc. In this work, we apply both vegetation indices and deep learning models on greenspace recognition. Our findings corroborate existing literature [8] in that deep learning which optimizes a nonlinear decision function with a large parameter set outperforms the thresholding vegetation indices.

2.2 Augmentation technique for deep learning-based vegetation analysis

Data augmentation is frequently used to increase training sample variety, which encourages deep learning model to learn discriminative and invariant image features. The strategy is effective to ease labeling requirement and improve model generalizability to predict on new unseen samples. Generic augmentation techniques for image recognition include geometric transformation, random color manipulation, edge enhancement, sharpening and blurring [82]. Though these techniques can apply to vegetation analysis, there is much flexibility and advantage to customize augmentation based on specific challenges in the domain. For example, graphically modelling for plant topology to generalize training sample to real plant distribution [92, 87], augmented image segments that focus on diseased spots for coffee plant disease identification [53], individual tree object augmentation for forest segmentation [44]. Color space transformations are explored to better discriminate plant to soil, but the analysis approach is based on simple linear and logarithmic functions [68]. Color augmentation is also used in deep learning model training for medical image and other general image types [49, 77, 66]. A common approach is color jitter [65], in which the brightness, contrast, saturation, and hue of an image is randomly changed to let the model learn features invariant to these image properties [82, 63]. Though the approach is practical to implement, arbitrary color transformations on satellite images might simulate unrealistic data, such as grey or blue greenspace pixels, thus negatively affecting model learning. Motivated by the previous studies, we propose to augment data while maintaining important color properties of greenspace. We expand the training samples regarding the green hue in the HSV color space to alter the shades of green within a range, which improves deep learning model adaptation to various greenspace appearances.

Distinction from prior work. Our work stands out in the literature of both semantic segmentation algorithm and greenspace quantification for Karachi. First, we propose to leverage deep learning to quantify greenspace from satellite images, which surpasses the gold standard vegetation index methods in performance. We also further improve model segmentation performance by tackling the existing class imbalance problem, that Karachi satellite images include much fewer greenspace pixels

Table 1. Our work compared to prior related work in methodology (blue) and application (red) aspects.

	Vegetation index [62, 34, 57]	Deep learning [19, 74, 108]	ColorJitter and GaussianNoise [65]	Focal Loss [75, 40, 99]	**Our work**
Augmentation method used	NA (No training).	Basic geometric transformations including random rotation, horizontal flip and vertical flip.	Basic geometric and color space transformations: random change of brightness, contrast, saturation and hue. Gaussian noise injection.	Basic geometric transformations.	Basic geometric transformations, and green color transformation: random change of green hue.
Training loss used	NA (No training).	Cross entropy loss for pixel-wise predictions.	Cross entropy loss.	Cross entropy with a weighting factor to tackle class imbalance.	Cross entropy loss.
Segmentation performance	Dependence on reflectance features and inability to detect greenspace variations.	Automated feature extraction and ability to capture complex patterns.	Improvement obtained from additional color augmentation (0.4-1.7% increased IoU) or noise injection (0-2.3% increased IoU).	Improvement obtained by balancing loss for greenspace class (0.7% increased IoU).	Most performance gain by adapting model to green hue variations (15% increased IoU).
	Qureshi et al. [71]	Ghazal et al. [33]	Batool et al. [10]	Arshad et al. [4]	**Our work**
Study area in Karachi	3 selected urbanization sites	1 open space in Karachi	Urban area at southern Karachi	Urban area at southern Karachi	Whole area of Karachi
Data collected to quantify greenspace	Questionnaire survey	Satellite image data in 0.6 and 30 meter resolution	Satellite image data in 30 meter spatial resolution	Governmental land use and land cover data	Satellite image data in 0.27 meter resolution

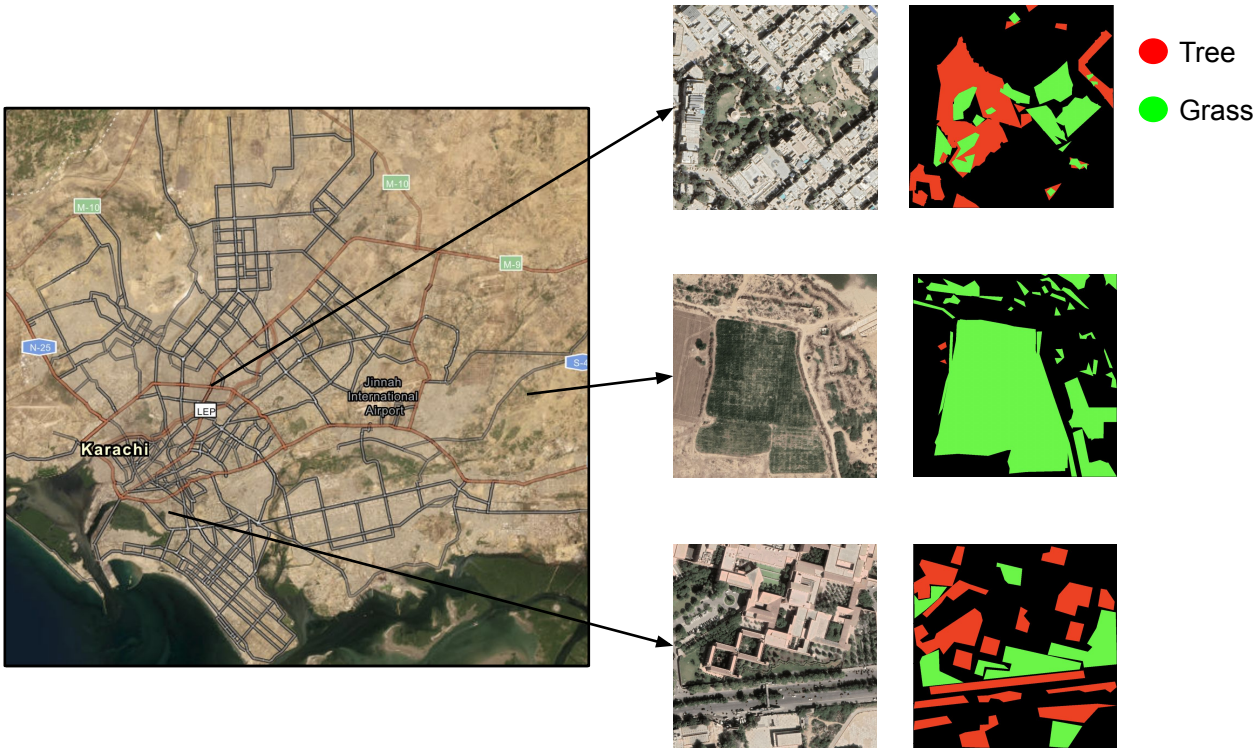

Figure 1. Examples of three satellite images (1024 $\times$ 1024 pixels, 0.27 m/pixel) and manually labeled greenspace masks. We download satellite data covering the whole Karachi city and select 620 image tiles for labeling. (The map: ©OpenStreetMap contributors, TomTom, Garmin, Foursquare, METI/NASA, USGS).

than background. Our method outperforms state-of-the-art methods for this problem, including using augmentation and regularization loss. Second, we perform analyses of greenspace distribution across the whole area of Karachi, using collected high resolution satellite images, in comparison to previous work which has only studied limited areas in Karachi. Table 1 summarizes these distinctions.

3 Method

3.1 Study area

The study location is Karachi, the largest city in Pakistan (has an area of 3,530 km^2)[2], and population of over 17 million[3]. The analysis unit is union council (n=173), the fifth (lowest) level of government in Pakistan. The extent shows a need to quantify greenspaces at a high resolution covering Karachi for effective urban planning and sustainability [13, 73]. Being a metropolitan city, Karachi faces a huge influx of urbanization and industrialization and ranks as the third largest city in

[2]City K-OWPoKM. Karachi the Gateway to Pakistan. http://www.kmc.gos.pk/contents.aspx?id=14
[3]World Population Review. https://worldpopulationreview.com/world-cities/karachi-population

Table 2. Distribution of labels for each class in the training dataset. The dataset is heavily imbalanced that the greenspace classes to recognize have low representation.

Class	Pixel count	Frequency
Background	4.53×10^8	0.697
Tree/Shrub	1.24×10^8	0.190
Grass	7.34×10^7	0.113

the world with respect to population, as of 2018[4]. These challenges combined pose a threat to resources and environment in the city, most susceptible being the green and open spaces [72]. Indeed, Karachi's green areas have decreased by 4%, whereas the urban extent in the core city has expanded by 8% between 2005 and 2017 [1]. The tropical climate with hot arid summers and short dry winters also creates difficulty in maintenance of urban green spaces. Surveys conducted in Karachi show that more than half of the respondents rarely or never visit city natural spaces and they express concerns about lack of maintenance and public conveniences in and around greenspaces [72]. In sum, there is an urgent need of comprehensive greenspace measurement for city planning to maintain the quality of life and socio-environmental sustainability in Karachi.

3.2 Satellite data and annotation

We collected satellite images using the Application Programming Interfaces (APIs) from Google Maps Platform, consisting of aerial views of Karachi with a resolution of 0.27 m/pixel. The resulting number of images was 42,735, comprehensively covering the full area of 173 Union Councils across the city (3,530 km^2). Each image was 1024 $\times$ 1024 pixels, equivalent to 23,104 m^2 on the ground. The area of images with annotation is about 14.32 km^2; We labeled 620 acquired images manually, pixel-wise, to identify areas covered by trees, shrubs, and grass using the Labelbox tool[5]. Among them 400 images were selected randomly across the Karachi area, and another 220 images with large greenspace areas were selected to increase observation of the vegetation classes. The 620 annotated images are randomly split into a training/validation set with 80% of the images, and testing set with 20% of the images.

To ensure label quality, two members of the research team each labeled each image and the union was obtained. Labels were validated by a third reviewer to ensure no obvious greenspace areas are missed or labeled incorrectly. The label consensus for shrub areas was relatively low because of its similarity to trees, given that plant height is hard to estimate from the aerial view. Since woody vegetation is usually studied as one biodiversity component [79, 84], following the literature of building deep learning models to recognize mixed tree and shrub landcover [35, 95, 28], we merged the shrub labels into tree labels for the following analysis. The final class distributions are presented in Table 2. Satellite view of the study area and example greenspace annotations are shown in Fig. 1.

Population data of Karachi for computing per capita greenspace was obtained from Meta High Resolution Population Density Map[6]. The map provides 2020 population statistics with geo-coordinates for grid units around the world at a 30 m resolution. We compute the population sum of units located in each Karachi union council as the population distribution of

[4]Largest cities in the world CITYMAYORS STATISTICS2018. http://www.citymayors.com/statistics/largest-cities-population-125.html.
[5]Labelbox. https://labelbox.com/
[6]https://dataforgood.facebook.com/dfg/tools/high-resolution-population-density-maps

the city.

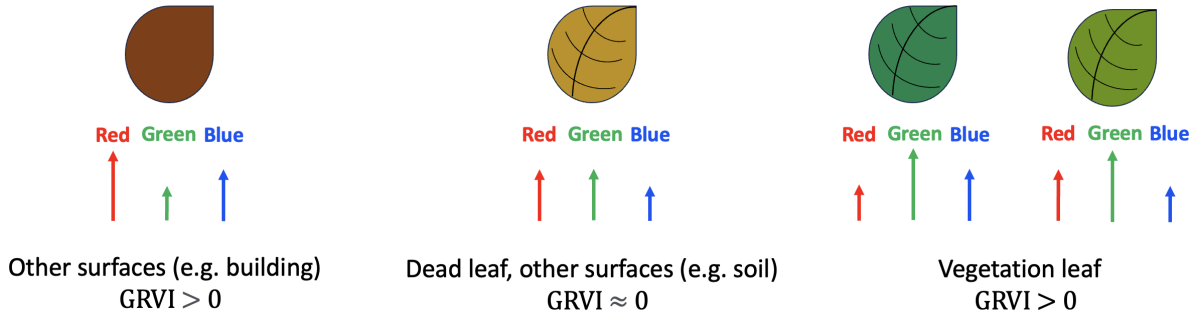

Figure 2. The overview of how vegetation index GRVI measures the difference between red and green reflectance (indicated by the arrows), to differentiate vegetation and non-vegetation surface with a index value threshold (GRVI>0).

3.3 Analysis

3.3.1 Visible band vegetation indices

Vegetation index methods can directly analyze greenspace based on the image RGB channel value, computed via their equations and a threshold parameter. The output of each index is a binary prediction: vegetation or non-vegetation, for each image pixel. Three visible band vegetation indices are used: (1) green-red vegetation index (GRVI), based on the contrast between reflectance in green and red bands of green vegetation ground cover [62]; (2) visible atmospheric resistant index (VARI), which reduces atmospheric effects by including the blue band [34]; and (3) green leaf index (GLI), proposed for wheat cover estimation [57]. The equations for the indices are:

$$GRVI = (\rho_{green} - \rho_{red})/(\rho_{green} + \rho_{red}) \tag{1}$$

$$VARI = (\rho_{green} - \rho_{red})/(\rho_{green} + \rho_{red} - \rho_{blue}); \tag{2}$$

$$GLI = (2\rho_{green} - \rho_{red} - \rho_{blue})/(2\rho_{green} + \rho_{red} + \rho_{blue}). \tag{3}$$

, where ρ_c is the reflectance value of the visible band in color c. Example images and corresponding GRVI values are shown in Fig. 2. Healthy vegetation reflects more green light than red light due to chlorophyll, resulting in a positive GRVI value, while unhealthy or non-vegetative surfaces often reflect less green light than red light, resulting in a GRVI closer to zero or negative values. The other indices use a similar method to identify vegetation based on relative reflectance of visible bands, and have also shown to be useful vegetation indicators [62, 5, 38].

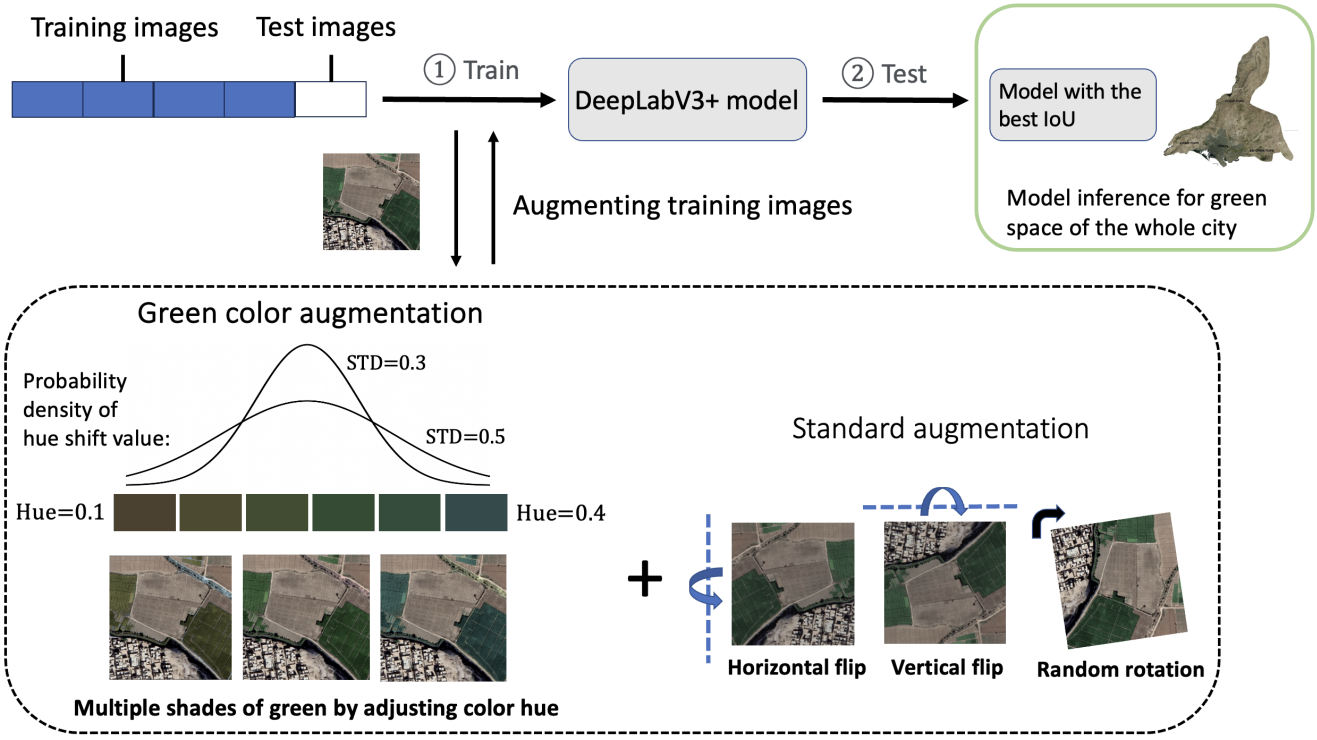

Figure 3. The overview of developing green color augmentation for deep learning based greenspace segmentation: The model DeepLabV3+ is trained on 80% of the labeled images, the training set, with schedules and hyper-parameters fine-tuned. Trained models are tested on 20% of the labeled images and the model which obtains the best Intersection over Union (IoU) is selected to analyze the distribution of overall greenspace and different vegetation types across the city. Illustration of green color augmentation method during training: The green hue of images is shifted with a value randomly selected from a normal distribution, to simulate new greenspace patterns. This custom augmentation is used in addition to traditional image augmentations including random flip, rotation and cropping.

3.3.2 Deep learning model and setup

Encoder-decoder structural models are commonly used for deep learning based semantic segmentation [7, 19, 26, 59, 51]. The encoder produces low resolution and high semantic representations from images, and the decoder maps the representation to pixel-level class predictions [19]. We apply DeepLabV3+, a deep convolutional neural network that follows the encoder-decoder architecture. The DeepLab model family is known for using dilated convolution for larger receptive fields, and conditional random fields to refine segmentation boundary, thus achieving enhanced segmentation performance. DeepLabV3+ makes further improvement by applying dilated convolution at multiple scales and flexible encoder feature resolutions [19]. This model has achieved state-of-the-art semantic segmentation performance for vegetation detection and classification [6, 5, 17, 23]. In contrast to vegetation indices, the deep learning approach can distinguish greenspace classes, thus here is also trained to identify the greenspace types, trees and grass.

We follow the standard protocol for training deep segmentation model as used in [109]. Input images are randomly cropped into the size of 512×512 with a batch size of 16. Image augmentations including random horizontal flip, vertical flip, and rotation for 90 degrees are applied. The loss function is pixel-level cross entropy which measures model prediction error and a stochastic gradient descent (SGD) optimizer minimizes the error by updating model weights. The initial learning rate is 10^{-3} with a momentum of 0.9 and a weight decay of 10^{-4}. The learning rate is decayed during training using a polynomial learning rate scheduler implemented in PyTorch [65]. The model is trained and validated for 100 epochs and final performance is evaluated on the test images. An overview of the training pipeline is shown in Fig. 3.

3.3.3 Green color augmentation for vegetation detection

A challenge for greenspace detection in real-world situations is the non-uniformity of colors. For example, some shrubs or grass may have a straw yellow or pale brown appearance, which are less distinguishable from non-vegetation objects. Accordingly, to train the deep learning model to recognize the multitude of vegetation patterns, we design a simple but effective data augmentation method; by shifting the hue value of the original images, new images are generated which depict the same vegetation objects but with a new color. The augmented images reduce the deep learning model's over-fitting to the training data and increase generalizability to different shades of green. Importantly, the augmentation does not impact the semantic (content) information of the original images; it only operates on the greenspace regions and the hue value change is restricted to a reasonable range. For example, when changing the hue from 0.1 to 0.4, the color of the grass region changes from olive green to dark green. The process is visualized in Fig. 3 (bottom left).

Algorithmic steps of the green color augmentation are to: 1) Convert the RGB image into HSV (hue, saturation, value) format. 2) Produce a random hue shift Z following a normal distribution, which has the mean of 0 and standard deviation of σ. A bigger σ indicates a higher probability to apply large hue shifts, which can be understood as "augmentation strength". We choose randomized hue shifts during training instead of fixed values to maximize the variety of simulated colors. The setting of $Z \sim \mathcal{N}(0, 1.0^2)$ obtains the best results for the Karachi data used in this work, and the method's sensitivity to different σ parameters are analyzed in Fig. 5. 3) Define the range of green hue $[h_l, h_r]$ of greenspace pixels in the whole dataset. 4) Apply Z to the hue value of pixels labeled as greenspace, within the range $[h_l, h_r]$. As a result, the adjustment for

a pixel with hue value h_i will be as follows:

$$h_i = \begin{cases} h_i + max\{Z, h_r - h_i\}, & \text{if } Z > 0 \\ h_i + max\{-Z, h_i - h_l\}, & \text{if } Z < 0. \end{cases} \tag{4}$$

Finally, the augmented images with the new hue values are converted back into RGB format. The images are further processed with standard augmentation functions to be input to the model.

3.4 Detection of roads and their relationship to greenspaces

We use a pre-trained road extraction model, D-LinkNet [108], to quantify road distribution in Karachi. The model can detect paved road from high resolution satellite images and achieved the first place performance in the DeepGlobe 2018 Road Extraction Challenge [25]. During the inference, we use the parameters as in the original model to assign binary predictions for whether each pixel belongs to the road class. We compute the area of predicted road pixels since road length or area is a key measure for urban form [24]. Also following [24], we examine the relationship between road area and the quality of greenspace in terms of per capita greenspace, evaluated by Pearson's correlation coefficient at the union council level.

3.5 Retrieval of land surface temperature (LST) and its relationship to greenspace

We collect LST data from the MODIS11A1 satellite data product with a 1-km spatial resolution [90]. The mean LST for the two-year period 2021-2022 is computed because the used satellite data for greenspace analysis is downloaded during this time [7]. Moreover, the impact of greenspace on LST has been typically studied with year as the temporal unit [85, 9, 41, 43]. To perform bivariate relationship analysis between greenspace coverage and LST for local climate zone, we study the 13 union councils which each has area with available data larger than 10 km^2. For each union council, satellite images are divided into 1000 m $\times$ 1000 m tiles to align with LST data resolution. Greenspace coverage and mean LST are computed for each tile, and Pearson correlation coefficient is used to quantify their relationship.

4 Results and discussion

4.1 Model performance in binary and multi-class segmentation

Segmentation performance of vegetation index methods and deep learning methods are evaluated on the testing split of labeled images. For the first task of greenspace detection, vegetations (e.g. trees, grass) are combined into a single greenspace class and each image is segmented by pixel-wise binary (greenspace or not) classification. For the second task of segmenting different vegetation types, each image pixel is classified into one of the three classes: trees, grass, or background. The tree class groups all woody plants including lower shrubs, as motivated in Section 3.2. The second task is not feasible using vegetation indices.

[7] Satellite image acquisition date from Map Static API is not publicly available.

Table 3. Comparison of vegetation indices, baseline deep learning method DeepLabV3+, existing deep learning methods that tackle class imbalance, and our proposed method DeepLabV3+ (GreenAug). Segmentation tasks include binary prediction (Vegetation is "All"), and multi-class prediction by vegetation types (only for deep learning methods). Evaluation metrics and results are all class-wise.

Vegetation index	Vegetation	Recall ↑	Precision ↑	IoU ↑	Accuracy ↑
GRVI	All	0.573	0.588	0.393	0.643
VARI	All	0.442	0.721	0.371	0.696
GLI	All	0.633	0.640	0.466	0.669
Deep learning	**Vegetation**	**Recall ↑**	**Precision ↑**	**IoU ↑**	**Accuracy ↑**
DeepLabV3+	All	0.821	0.855	0.721	0.872
	Trees	0.714	0.828	0.621	0.905
	Grass	0.772	0.698	0.579	0.936
DeepLabV3+ (FL)	All	0.863	0.832	0.735	0.899
	Trees	0.737	0.819	0.634	0.909
	Grass	0.805	0.704	0.601	0.940
DeepLabV3+ (DFL)	All	0.843	0.840	0.726	0.896
	Trees	0.744	0.823	0.641	0.911
	Grass	0.712	0.781	0.593	**0.945**
DeepLabV3+ (UFL)	All	0.858	0.830	0.730	0.897
	Trees	0.741	0.813	0.633	0.909
	Grass	0.806	0.693	0.594	0.942
DeepLabV3+ (ColorJitter)	All	0.834	0.846	0.724	0.897
	Trees	0.712	0.841	0.627	0.911
	Grass	0.740	0.742	0.589	0.934
DeepLabV3+ (GaussianNoise)	All	0.833	0.844	0.721	0.896
	Trees	0.757	0.798	0.635	0.907
	Grass	0.720	0.776	0.596	**0.945**
DeepLabV3+ (GreenAug)	All	0.894	0.906	**0.828**	**0.927**
	Trees	0.774	0.857	**0.685**	**0.926**
	Grass	0.777	0.759	**0.623**	0.941

4.1.1 Comparison methods

We compare our proposed green color augmentation "DeepLabV3+ (GreenAug)" to vegetation indices and other relevant deep learning methods. The deep learning methods considered are: (1) A baseline semantic segmentation model "DeepLabV3+". In this model, as with *all* deep learning methods in this study, geometric augmentations, random flipping, rotation and cropping are applied, as these are standard practices for training a deep learning model [19]. (2) Color jitter augmentation [65], "DeepLabV3+ (ColorJitter)", by randomly shifting color space attributes. (3) Gaussian noise augmentation, "DeepLabV3+ (GaussianNoise)", by adding random values in normal distribution to the original pixel values [65]. Other augmentation methods as surveyed in [3, 97, 78] use generative models to simulate new images by background replacement, texture transfer, etc. These methods need separate training procedures to learn the deep generative models. Moreover, such existing methods focus on individual object recognition in which context and background are irrelevant, different to our task which requires a holistic understanding of the image, so the methods are not included. We also compare to (4) focal loss, "DeepLabV3+ (FL)" [75], which gives increased weight to hard mis-classified pixels, (5) dual focal Loss, "DeepLabV3+ (DFL)" [40], which resolves the vanishing gradient limitation of focal loss, and (6) unified focal loss, "DeepLabV3+ (UFL)" [99], which combines Dice loss to cross entropy-based loss used in focal loss. These loss functions have been proposed to handle class imbalance challenges in image segmentation.

4.1.2 Evaluation metrics

We evaluate greenspace segmentation models by segmentation completeness (recall), purity (precision), and overall segmentation quality, measured by the intersection of ground-truth masks and the predicted segmentation divided by their union (IoU). We additionally report pixel-level classification accuracy (accuracy). The metrics are defined based on TP, FP, TN, and FN, which are pixel-wise true positives, false positives, true negatives and false negatives for classifying greenspace:

$$\text{recall} = \frac{TP}{TP + FN} \tag{5}$$

$$\text{precision} = \frac{TP}{TP + FP} \tag{6}$$

$$\text{IoU} = \frac{TP}{TP + FP + FN} \tag{7}$$

$$\text{accuracy} = \frac{TP + TN}{TP + FP + FP + FN} \tag{8}$$

4.1.3 Results.

As reported in Table 3, deep learning methods largely outperform the vegetation indices on all metrics. DeepLabV3+ (GreenAug) segments 89.4% of the true greenspace, and has the correct rate of 90.6% of its predictions, while the best

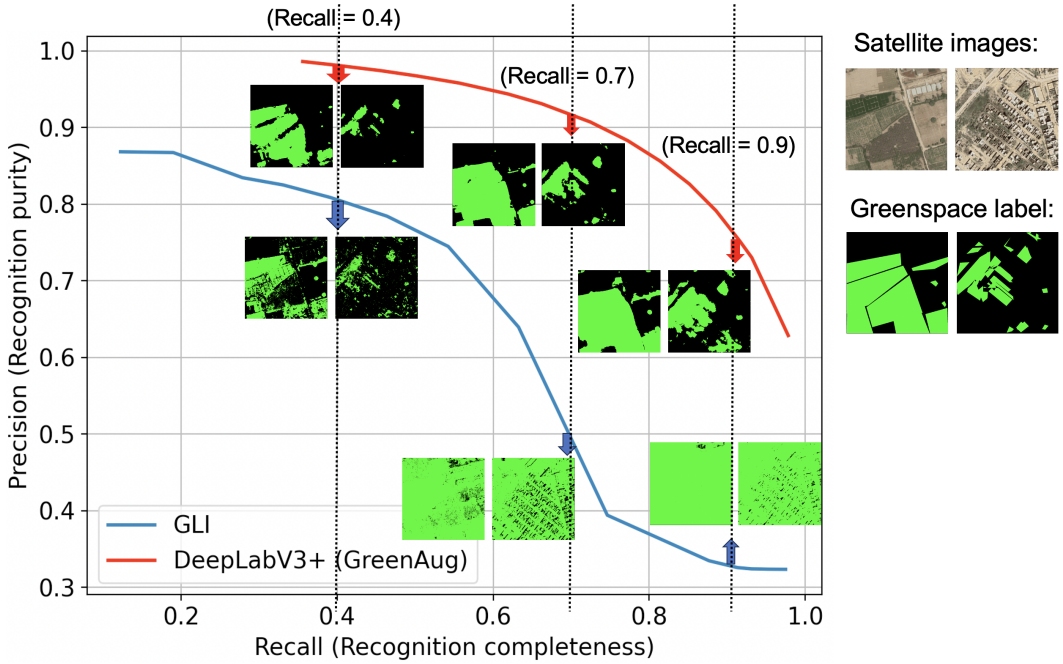

Figure 4. The precision and recall metric trade-off for greenspace segmentation, using vegetation index GLI and deep learning method DeepLabV3+ (GreenAug). Green pixels represent greenspace and black pixels represent background. Deep learning model can extract more discriminative features under prediction thresholds for different binary greenspace classification. Example images and segmentation results with the two methods are visualized, at the recall value of 0.4, 0.7, and 0.9. With the same recognition completeness, DeepLabV3+ (GreenAug) method obtains much higher recognition precision.

vegetation index method, green leaf index (GLI), segments 63.3% of the greenspace and 64.0% of its predictions are correct. Besides, the proposed DeepLabV3+ (GreenAug) obtains IoU=0.828 in segmenting all greenspace. Our method outperforms other deep learning methods that tackle class imbalance and under-representation by 13%-15% on greenspace segmentation IoU, though they have all improved the vanilla baseline. This comparison indicates that for domain specific applications, designing methods to incorporate domain information, such as to augment vegetation's green appearance that differs across growing conditions and environments in this task, can be more effective than general-purpose methods.

For the task of segmenting different vegetation species, as shown in Table 3, DeepLabV3+ (GreenAug) improves the segmentation IoU by 10.3% for trees class, 7.60% for grass class compared to the baseline DeepLabV3+ training with no optimization. It also outperforms other deep learning methods by 6.86%-10.3% for Trees, and 3.66%-7.60% for grass. Note that DeepLabV3+ (DFL) and DeepLabV3+ (GaussianNoise) obtain highest accuracy for grass (Accuracy=0.945). Improved accuracy can result because the accuracy metric measures pixel-wise classification for both background and greenspace classes. Since in these images the proportion of background pixels is much higher than grass pixels, methods that predict most pixels of an image as background obtain a high accuracy. This is reflected by the low recall and IoU for grass for those methods with a higher accuracy. Therefore, for highly underrepresented classes like grass, which constitutes only 11.3% of the training samples (versus 19.0% for trees and 30.3% for greenspace), the metric IoU better indicates segmentation performance than Accuracy. In sum, DeepLabV3+ (GreenAug) shows clear advantage via higher segmentation quality evaluated by IoU, resulting from improved recall. Overall, this model can capture greenspace features more completely, which instructs the model to better distinguish greenspace from other land covers.

4.2 Model precision and recall trade-off

Given that classification accuracy, precision and recall can vary by the threshold used for classifying greenspace versus others, we examine the segmentation performance at different pixel-wise classification decision thresholds (Fig. 4). Increasing the threshold for the GLI method improves recognition of outlier greenspace pixels such as vegetation with moss green appearance (which can have abnormal index value of red reflectance higher than green reflectance), thus improving recall. However, this increase simultaneously increases irrelevant background predictions and causes worse precision. The DeepLabV3+ (GreenAug) model shows a similar trend but has consistent higher performance. As shown by the example images when the two methods obtain the same recall of 0.4, 0.7, and 0.9, DeepLabV3+ (GreenAug) always recognizes more relevant greenspace pixels and has higher precision. This consistent improved performance shows the advantage of the deep learning method in real-world applications where different choices of thresholds are often set for detecting different types of greenspace.

4.3 Model sensitivity and robustness analysis

We investigate how the main parameter, the standard deviation σ used to generate random hue shift, affects model performance. As shown in Fig. 5 (left), when $\sigma = 0$, hue shift is 0 and the result is same as the baseline training with only standard augmentations applied. When increasing σ to use higher augmentation strength, model performance keeps improving until

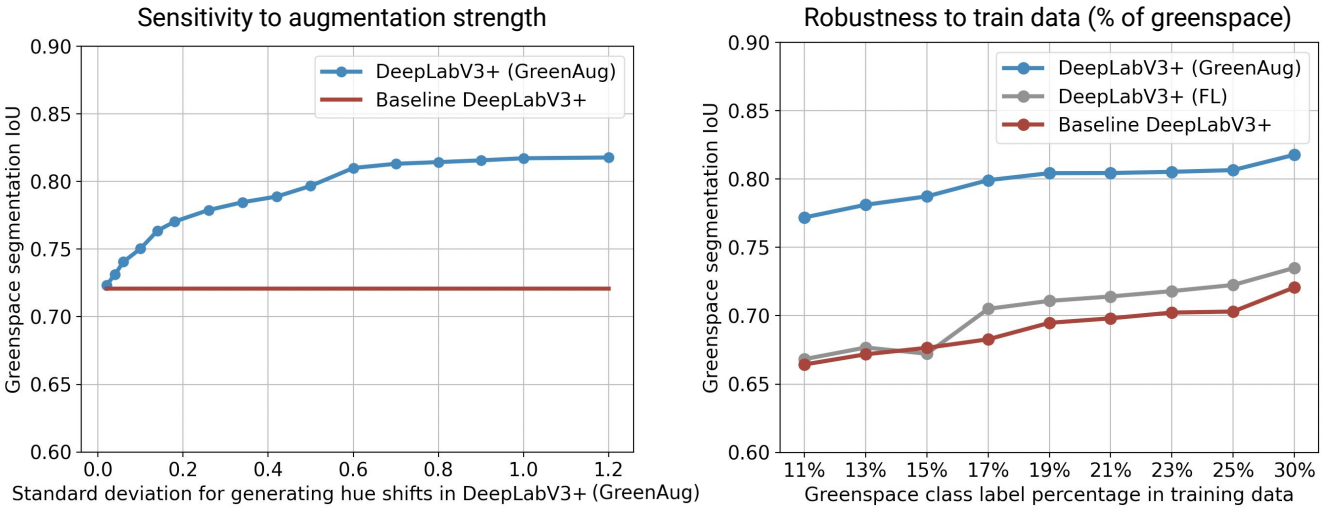

Figure 5. Graphs showing IoU score for greenspace class semantic segmentation, using the proposed augmentation method: DeepLabV3+(GreenAug), focal loss to upweight difficult samples: DeepLabV3+(FL), and only standard augmentations without any optimization for class imbalance: Baseline DeepLabV3+. Left; We test different values of the hue shift parameter σ used in the green color augmentation method DeepLabV3+ (GreenAug) and observe improvements over Baseline DeepLabV3+. Right; Different subsets of training data are used to train the model. Each subset has different greenspace label percentages, i.e., class imbalance degrees. The proposed method presents consistent advantages over Baseline DeepLabV3+ and DeepLabV3+(FL) under various training data distributions.

Table 4. Comparison of the baseline deep learning segmentation model UNet, the model applied with previous methods that tackle class imbalance, and the model applied with our proposed augmentation method UNet (GreenAug). Segmentation tasks include binary prediction (Vegetation is "All"), and multi-class prediction by vegetation types.

Deep learning	Vegetation	Recall ↑	Precision ↑	IoU ↑	Accuracy ↑
UNet	All	0.835	0.847	0.725	0.897
	Trees	0.785	0.791	0.650	0.910
	Grass	0.691	0.810	0.595	0.937
UNet (FL)	All	0.831	0.856	0.729	0.899
	Trees	0.775	0.811	0.656	0.914
	Grass	0.745	0.751	0.597	0.944
UNet (DFL)	All	0.866	0.829	0.735	0.899
	Trees	0.805	0.794	0.666	0.914
	Grass	0.739	0.765	0.602	0.944
UNet (UFL)	All	0.849	0.836	0.728	0.897
	Trees	0.801	0.794	0.663	0.914
	Grass	0.769	0.737	0.603	0.943
UNet (ColorJitter)	All	0.840	0.849	0.731	0.899
	Trees	0.769	0.811	0.652	0.913
	Grass	0.761	0.748	0.605	0.944
UNet (GaussianNoise)	All	0.830	0.853	0.727	0.898
	Trees	0.801	0.783	0.655	0.910
	Grass	0.736	0.776	0.607	0.944
UNet (GreenAug)	All	0.894	0.898	**0.811**	**0.920**
	Trees	0.824	0.828	**0.703**	**0.918**
	Grass	0.735	0.780	**0.609**	**0.945**

Table 5. Comparison of the baseline deep learning segmentation model LinkNet, the model applied with previous methods that tackle class imbalance, and the model applied with our proposed augmentation method LinkNet (GreenAug). Segmentation tasks include binary prediction (Vegetation is "All"), and multi-class prediction by vegetation types.

Deep learning	Vegetation	Recall ↑	Precision ↑	IoU ↑	Accuracy ↑
LinkNet	All	0.845	0.841	0.728	0.863
	Trees	0.751	0.809	0.638	0.884
	Grass	0.691	0.807	0.593	0.917
LinkNet (FL)	All	0.839	0.847	0.729	0.899
	Trees	0.782	0.789	0.647	0.909
	Grass	0.714	0.785	0.597	**0.946**
LinkNet (DFL)	All	0.848	0.843	0.732	0.899
	Trees	0.765	0.814	0.651	0.913
	Grass	0.751	0.758	0.606	0.945
LinkNet (UFL)	All	0.856	0.818	0.719	0.893
	Trees	0.765	0.803	0.644	0.910
	Grass	0.735	0.775	0.605	0.945
LinkNet (ColorJitter)	All	0.838	0.847	0.728	0.898
	Trees	0.762	0.812	0.648	0.912
	Grass	0.747	0.770	0.610	**0.946**
LinkNet (GaussianNoise)	All	0.843	0.842	0.727	0.897
	Trees	0.768	0.799	0.643	0.909
	Grass	0.747	0.766	0.608	0.944
LinkNet (GreenAug)	All	0.888	0.895	**0.805**	**0.930**
	Trees	0.807	0.827	**0.691**	**0.921**
	Grass	0.771	0.810	**0.653**	0.941

reaching a plateau at approximately $\sigma = 1.0$. This value and the overall sensitivity of green color augmentation to σ should be affected by specific greenspace color distribution in different datasets. Thus, we further analyze the robustness of the augmentation method to dataset composition, i.e., if the method is effective on training images with more scarce greenspace labels. Fig. 5 (right) illustrates segmentation performance for 11% to 30% target labels, by selecting subsets of the training images and evaluating on the same set of testing images. The proposed method maintains its advantage over the baseline methods throughout different training label volumes.

Additionally, We validate robustness of the proposed green color augmentation method across different segmentation architectures. We apply the method on two additional deep learning model architectures, UNet [74] and LinkNet [15], used in previous work for segmenting greenspace [42, 23, 55]. The models use the same encoder-decoder structure for segmentation as DeepLabV3+ but with variations in feature extraction procedure. Comparison results in Table 5 show that our augmentation method is generalizable to different segmentation models and achieves improved performance on all metrics.

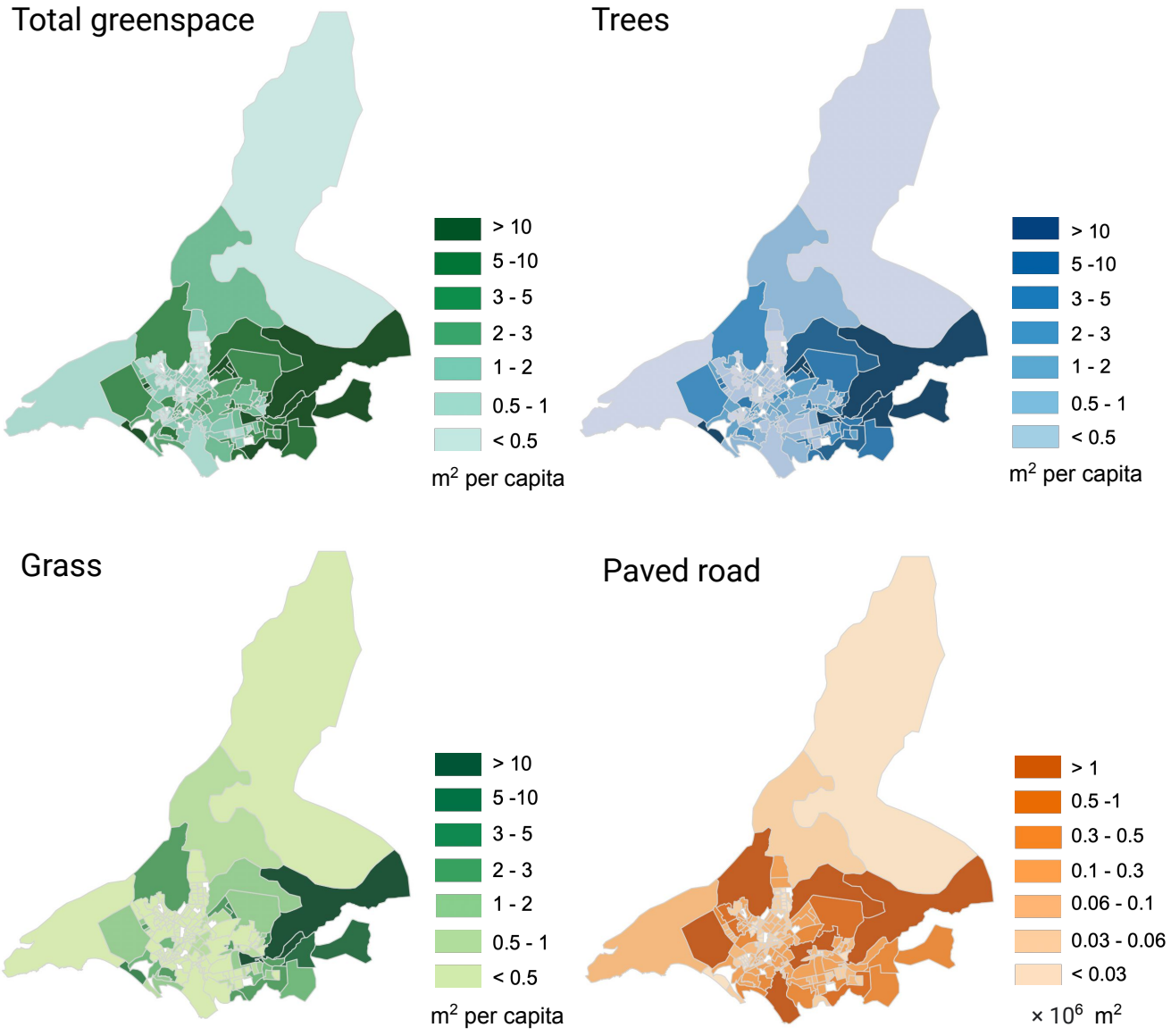

Figure 6. Spatial distribution of total greenspace, trees, and grass per capita, and areas of paved road in Karachi, union councils.

Table 6. Pearson's correlation coefficient (PCC) between greenspace coverage and land surface temperature (LST) for large union councils. *** $p < 0.01$, ** $p < 0.05$, * $p < 0.1$.

Union council	Rehri	Cattle Colony	Murad Memon	Malir Cantonment
PCC	-0.727 ***	-0.661 **	-0.791 ***	-0.334 *
Union council	Baba Bhitt	Mango Pir	Songal	Landhi
PCC	-0.567 **	-0.566 ***	-0.269 **	-0.491 *

4.4 Downstream analyses - greenspace relates to economic and climate factors

The proposed deep learning method is used to label images across all of Karachi, and compute two values. First, as an overall examination of greenspace amount and availability in the city, we compute per capita greenspace. The World Health Organization (WHO) recommends a minimum of 9 m^2/capita of greenspace per individual with an ideal value of 50 m^2/capita [76]. Using our method, we find that the mean per capita greenspace across union councils (smallest administrative level in Karachi) is 4.17 m^2/capita. The greenspace availability also varies highly across union councils; 3 union councils have the highest greenspace values of over 80 m^2/capita (Darsanno Channo, Murad Memon, and Gulshan-e-hadeed), while 5 union councils have the lowest values of less than 0.1 m^2/capita (Darya Abad, Behar Colony, Chushti Nagar, Banaras Colony, and Gulshan Said). We note that the areas where per capita greenspace is higher than the World Health Organization recommendations are mostly on the periphery of Karachi (Fig. 1), especially the eastern region. The region has rich surface water resources and collects most cultivated areas [46]. Therefore, the union councils located there are less populated and occupied by large agricultural lands or wild forests, showing high per capita greenspace. Moreover, we compute specific greenspace types per capita predicted by the trained multi-class semantic segmentation model. As shown in Fig. 1, the spatial distribution of trees and grass have a similar pattern to the total greenspace.

Next, to understand where greenspaces are located, we examine the greenspace area by union council in comparison to a measure of economic development and urbanization, paved roads [64, 70]. Pearson's correlation coefficient reveals that per capita greenspace has a significant positive correlations with paved road area (0.352, $p < 0.001$), and by vegetation type, there is a higher correlation for the tree greenspace type (0.367, p <0.001), versus grass (0.233, p <0.01). The map in Fig. 1 shows that road distributions have a similar spatial pattern with per capita greenspace. These results corroborate how road-side greenbelts are a main greenspace component in urbanized areas [110, 69]. Indeed, green infrastructures like parks and roads are often considered simultaneously in urban planning [37].

We also explore the potential benefit of understanding greenspace distribution by its role in thermal environment. Greenspace has been proven effective to mitigate urban heat island effects [36]. Indeed, for Pakistan, decreased greenspace is shown to relate to LST increase over years in multiple areas [93, 85, 9, 43]. Correlation between LST and greenspace coverage is measured at a level of 1 km^2 land (the resolution of the LST data) within each union council. The analysis is only performed for union councils which provide an area with enough data samples to perform a correlation analysis. The results are shown in Table 6; significant negative correlations are observed for 8 of the union councils, suggesting a thermal regulation where

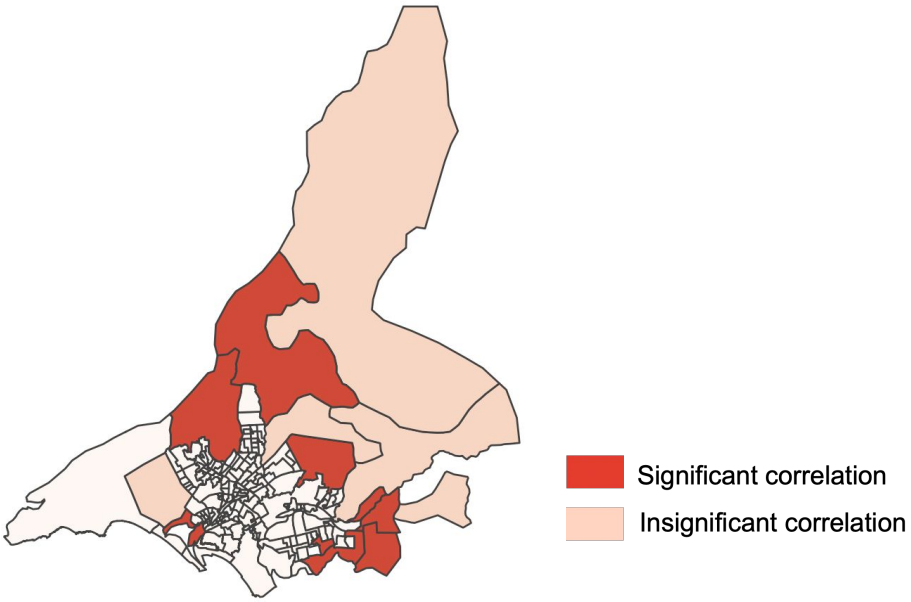

Figure 7. The location of union councils which each have data available in an area larger than 10 km^2. The color is coded by significance level, those in which greenspace has significant negative correlation to LST if $p < 0.1$, or else the correlation is insignificant.

there is more greenspace. The relationship varies across areas; Mauri Pur, Darsanno Channo, Gujjro, Gulshan-e-hadeed, and Gadap do not present significant correlation between greenspace coverage and LST. These areas are located at the periphery of the city, covered by mostly bareland. The location of the studied union councils are visualized in Fig. 7. Our findings agree with a previous study [9] which shows negative relationships between normalized difference vegetation index and normalized LST in part of the central urban areas of Karachi.

5 Limitations and future work

This work is not without limitations. Importantly, for the analysis of greenspace distribution, we focus on it only in comparison to road infrastructure, as we are limited by lack of availability of other socioeconomic data at comparable granular levels (i.e., union council). If other types of relevant data are available in the future, such as poverty indices or school locations at the level of Karachi union council, researchers can further study the accessibility or impact of greenspaces in Karachi. Further, we focus primarily on recognizing trees and grass in this work, limited by annotation costs. Future work may label the training data with different greenspaces types, for example, to divide the Tree class into Shrubs and Forest, and apply the developed augmentation method for their recognition. Another potential challenge is model generalization. Though the proposed augmentation strategy is model-agnostic, the greenspace segmentation model trained on Karachi satellite images may not produce equally accurate results on images from a different geographic area, if directly using the model to predict without fine-tuning. This challenge is well-studied in the machine learning literature, and is due to data distribution discrepancy between areas. Indeed, the model is expected to generalize better to areas with similar landscape characteristics to Karachi,

such as broader south Asia, than areas with discrepant landscapes such as Europe. To expand the Karachi greenspace segmentation model to different geographic areas, researchers can re-train a model with the proposed augmentation method on labeled satellite images from that area, or leverage domain adaptation methods [106, 111, 45] to transfer a pre-trained model on Karachi to predict on the target area.

6 Conclusion

In this work we first confirm that using visible-band satellite images, deep learning consistently outperforms vegetation indices for greenspace extraction [103, 29, 16]. This new approach has the benefit of resolving green spaces with high spatial granularity (e.g. single trees), as well as the ability to distinguish types of greenspace. The deep learning models consist of multiple convolutional neural network layers, providing a more complex functional form than the vegetation index, to capture features of greenspace such as vegetation object shapes, textures, colors, and other semantic visual cues through a high dimensional representation. Our new method further improves performance via a custom data augmentation step; data augmentation is commonly used in deep learning model training to increase image diversity. As the greenspace coverage is overall low in Karachi (there are only 1.65% greenspace pixels from the collected satellite images covering the city), data augmentation provides a specifically relevant step in order to avoid over-fitting on the limited greenspace patterns and losing accuracy on new unseen images. The augmentation paradigm we propose shows consistent improvement using it with different deep learning architectures, by increasing training data diversity with respect to the important feature for the application, the green hue of vegetation. Notably, the method requires no additional learning structure or GPU computing, thus it can be easily integrated into different pipelines. Robustness of our proposed method is also demonstrated based on using different proportions of images with greenspace pixels for training the model, showing its consistent advantage on datasets with limited greenspace representations or annotations. Our other contributions include using the method to audit the greenspace per capita in Karachi, and demonstrating current distribution of greenspace in the city.

Practically, the deep learning based method shown in this work can be used to understand greenspace and inform urban planning. First, we show the per capita greenspace in Karachi is below WHO recommendations. In comparison, Singapore, which is densely populated (8358 people/km^2), has planned and incorporated greenspaces within the urban environment, reaching the minimum recommended, with 9.9 m^2/capita illustrating the feasibility of this target with appropriate planning efforts. Future studies could build upon our method to recognize further greenspace types across different geographic regions by expanding the training data. Further, in places such as Karachi, our work shows that greenspace currently correlates with economically developed areas and reduced heat. Accordingly, there is a need to improve their prevalence in other parts of the city, using this information to better plan their development. Overall, the scale-able nature, high granularity and delineation of using deep learning and satellite images can be used to monitor and plan for such resources to be available for all communities. The benefit of greenspace quantification is to understand its relationship to other land features.

References

[1] A. Ahmed. Green areas in karachi decreased by 4pc from 2005 to 2017, says wb report, Feb 2020.

[2] B. Ahmed and R. Ahmed. Modeling urban land cover growth dynamics using multi-temporal satellite images: a case study of dhaka, bangladesh. *ISPRS International Journal of Geo-Information*, 1(1):3–31, 2012.

[3] K. Alomar, H. I. Aysel, and X. Cai. Data augmentation in classification and segmentation: A survey and new strategies. *Journal of Imaging*, 9(2):46, 2023.

[4] A. Arshad, M. Ashraf, R. S. Sundari, H. Qamar, M. Wajid, and M.-u. Hasan. Vulnerability assessment of urban expansion and modelling green spaces to build heat waves risk resiliency in karachi. *International journal of disaster risk reduction*, 46:101468, 2020.

[5] B. Ayhan, C. Kwan, B. Budavari, L. Kwan, Y. Lu, D. Perez, J. Li, D. Skarlatos, and M. Vlachos. Vegetation detection using deep learning and conventional methods. *Remote Sensing*, 12(15):2502, 2020.

[6] B. Ayhan, C. Kwan, J. Larkin, L. Kwan, D. Skarlatos, and M. Vlachos. Deep learning model for accurate vegetation classification using rgb image only. In *Geospatial Informatics X*, volume 11398, pages 130–143. SPIE, 2020.

[7] V. Badrinarayanan, A. Kendall, and R. Cipolla. Segnet: A deep convolutional encoder-decoder architecture for image segmentation. *IEEE transactions on pattern analysis and machine intelligence*, 39(12):2481–2495, 2017.

[8] J. E. Ball, D. T. Anderson, and C. S. Chan. Comprehensive survey of deep learning in remote sensing: theories, tools, and challenges for the community. *Journal of applied remote sensing*, 11(4):042609–042609, 2017.

[9] M. F. Baqa, L. Lu, F. Chen, S. Nawaz-ul Huda, L. Pan, A. Tariq, S. Qureshi, B. Li, and Q. Li. Characterizing spatiotemporal variations in the urban thermal environment related to land cover changes in karachi, pakistan, from 2000 to 2020. *Remote Sensing*, 14(9):2164, 2022.

[10] R. Batool, F. Sarwar, and K. Javid. Evaluating spatial patterns of urban green spaces in karachi, pakistan through satellite remote sensing techniques: Satellite remote sensing techniques. *Proceedings of the Pakistan Academy of Sciences: A. Physical and Computational Sciences*, 56(1):45–52, 2019.

[11] J. Bendig, K. Yu, H. Aasen, A. Bolten, S. Bennertz, J. Broscheit, M. L. Gnyp, and G. Bareth. Combining uav-based plant height from crop surface models, visible, and near infrared vegetation indices for biomass monitoring in barley. *International Journal of Applied Earth Observation and Geoinformation*, 39:79–87, 2015.

[12] S. Borelli, M. Conigliaro, F. Pineda, et al. Urban forests in the global context. *Unasylva*, 69(250):3–10, 2018.

[13] J. Breuste, J. Schnellinger, S. Qureshi, and A. Faggi. Urban ecosystem services on the local level: Urban green spaces as providers. *Ekológia (Bratislava)*, 32(3):290–304, 2013.

[14] D. Chai, S. Newsam, H. K. Zhang, Y. Qiu, and J. Huang. Cloud and cloud shadow detection in landsat imagery based on deep convolutional neural networks. *Remote sensing of environment*, 225:307–316, 2019.

[15] A. Chaurasia and E. Culurciello. Linknet: Exploiting encoder representations for efficient semantic segmentation. In *2017 IEEE visual communications and image processing (VCIP)*, pages 1–4. IEEE, 2017.

[16] D. Chen, F. Zhang, M. Zhang, Q. Meng, C. Y. Jim, J. Shi, M. L. Tan, and X. Ma. Landscape and vegetation traits of urban green space can predict local surface temperature. *Science of The Total Environment*, 825:154006, 2022.

[17] J. Chen, S. Shao, Y. Zhu, Y. Wang, F. Rao, X. Dai, and D. Lai. Enhanced automatic identification of urban community green space based on semantic segmentation. *Land*, 11(6):905, 2022.

[18] L.-C. Chen, G. Papandreou, F. Schroff, and H. Adam. Rethinking atrous convolution for semantic image segmentation. *arXiv preprint arXiv:1706.05587*, 2017.

[19] L.-C. Chen, Y. Zhu, G. Papandreou, F. Schroff, and H. Adam. Encoder-decoder with atrous separable convolution for semantic image segmentation. In *Proceedings of the European conference on computer vision (ECCV)*, pages 801–818, 2018.

[20] X.-L. Chen, H.-M. Zhao, P.-X. Li, and Z.-Y. Yin. Remote sensing image-based analysis of the relationship between urban heat island and land use/cover changes. *Remote sensing of environment*, 104(2):133–146, 2006.

[21] Y. Chen, Q. Weng, L. Tang, Q. Liu, X. Zhang, and M. Bilal. Automatic mapping of urban green spaces using a geospatial neural network. *GIScience & Remote Sensing*, 58(4):624–642, 2021.

[22] G. Cheng, Y. Wang, S. Xu, H. Wang, S. Xiang, and C. Pan. Automatic road detection and centerline extraction via cascaded end-to-end convolutional neural network. *IEEE Transactions on Geoscience and Remote Sensing*, 55(6):3322–3337, 2017.

[23] A. Dabra and V. Kumar. Evaluating green cover and open spaces in informal settlements of mumbai using deep learning. *Neural Computing and Applications*, pages 1–16, 2023.

[24] R. G. Davies, O. Barbosa, R. A. Fuller, J. Tratalos, N. Burke, D. Lewis, P. H. Warren, and K. J. Gaston. City-wide relationships between green spaces, urban land use and topography. *Urban Ecosystems*, 11:269–287, 2008.

[25] I. Demir, K. Koperski, D. Lindenbaum, G. Pang, J. Huang, S. Basu, F. Hughes, D. Tuia, and R. Raskar. Deepglobe 2018: A challenge to parse the earth through satellite images. In *Proceedings of the IEEE Conference on Computer Vision and Pattern Recognition Workshops*, pages 172–181, 2018.

[26] F. I. Diakogiannis, F. Waldner, P. Caccetta, and C. Wu. Resunet-a: A deep learning framework for semantic segmentation of remotely sensed data. *ISPRS Journal of Photogrammetry and Remote Sensing*, 162:94–114, 2020.

[27] E. Dinnie, K. M. Brown, and S. Morris. Reprint of "community, cooperation and conflict: Negotiating the social well-being benefits of urban greenspace experiences". *Landscape and urban planning*, 118:103–111, 2013.

[28] D. J. Dixon, Y. Zhu, C. F. Brown, and Y. Jin. Satellite detection of canopy-scale tree mortality and survival from california wildfires with spatio-temporal deep learning. *Remote Sensing of Environment*, 298:113842, 2023.

[29] G. Fu and W. Sun. Temperature sensitivities of vegetation indices and aboveground biomass are primarily linked with warming magnitude in high-cold grasslands. *Science of The Total Environment*, 843:157002, 2022.

[30] A. Galderisi and E. Treccozzi. Green strategies for flood resilient cities: The benevento case study. *Procedia environmental sciences*, 37:655–666, 2017.

[31] J. A. Gamon, K. F. Huemmrich, C. Y. Wong, I. Ensminger, S. Garrity, D. Y. Hollinger, A. Noormets, and J. Peñuelas. A remotely sensed pigment index reveals photosynthetic phenology in evergreen conifers. *Proceedings of the National Academy of Sciences*, 113(46):13087–13092, 2016.

[32] B.-C. Gao. Ndwi—a normalized difference water index for remote sensing of vegetation liquid water from space. *Remote sensing of environment*, 58(3):257–266, 1996.

[33] L. Ghazal, S. Zubair, J. H. Kazmi, and H. Ghani. Assessment of transformation of urban green spaces and agriculture land in karachi: A case study of gutter bagheecha in and its surrounding areas. *Int. J. Biol. Biotech*, 15(2):527–534, 2018.

[34] A. A. Gitelson, Y. J. Kaufman, R. Stark, and D. Rundquist. Novel algorithms for remote estimation of vegetation fraction. *Remote sensing of Environment*, 80(1):76–87, 2002.

[35] E. Guirado, S. Tabik, D. Alcaraz-Segura, J. Cabello, and F. Herrera. Deep-learning versus obia for scattered shrub detection with google earth imagery: Ziziphus lotus as case study. *Remote Sensing*, 9(12):1220, 2017.

[36] K. R. Gunawardena, M. J. Wells, and T. Kershaw. Utilising green and bluespace to mitigate urban heat island intensity. *Science of the Total Environment*, 584:1040–1055, 2017.

[37] W. Halecki, T. Stachura, W. Fudała, A. Stec, and S. Kuboń. Assessment and planning of green spaces in urban parks: A review. *Sustainable Cities and Society*, 88:104280, 2023.

[38] W. Hashim, L. S. Eng, G. Alkawsi, R. Ismail, A. A. Alkahtani, S. Dzulkifly, Y. Baashar, and A. Hussain. A hybrid vegetation detection framework: Integrating vegetation indices and convolutional neural network. *Symmetry*, 13(11):2190, 2021.

[39] M. Helbich, Y. Yao, Y. Liu, J. Zhang, P. Liu, and R. Wang. Using deep learning to examine street view green and blue spaces and their associations with geriatric depression in beijing, china. *Environment international*, 126:107–117, 2019.

[40] M. S. Hossain, J. M. Betts, and A. P. Paplinski. Dual focal loss to address class imbalance in semantic segmentation. *Neurocomputing*, 462:69–87, 2021.

[41] M. Hu, Y. Wang, B. Xia, and G. Huang. Surface temperature variations and their relationships with land cover in the pearl river delta. *Environmental Science and Pollution Research*, 27:37614–37625, 2020.

[42] R. E. Huerta, F. D. Yépez, D. F. Lozano-García, V. H. Guerra Cobián, A. L. Ferriño Fierro, H. de León Gómez, R. A. Cavazos González, and A. Vargas-Martínez. Mapping urban green spaces at the metropolitan level using very high

resolution satellite imagery and deep learning techniques for semantic segmentation. *Remote Sensing*, 13(11):2031, 2021.

[43] S. Hussain and S. Karuppannan. Land use/land cover changes and their impact on land surface temperature using remote sensing technique in district khanewal, punjab pakistan. *Geology, Ecology, and Landscapes*, 7(1):46–58, 2023.

[44] S. Illarionova, D. Shadrin, V. Ignatiev, S. Shayakhmetov, A. Trekin, and I. Oseledets. Augmentation-based methodology for enhancement of trees map detalization on a large scale. *Remote Sensing*, 14(9):2281, 2022.

[45] J. Iqbal and M. Ali. Weakly-supervised domain adaptation for built-up region segmentation in aerial and satellite imagery. *ISPRS Journal of Photogrammetry and Remote Sensing*, 167:263–275, 2020.

[46] M. Irfan, S. J. H. Kazmi, and M. H. Arsalan. Sustainable harnessing of the surface water resources for karachi: a geographic review. *Arabian Journal of Geosciences*, 11:1–11, 2018.

[47] J. John, G. Bindu, B. Srimuruganandam, A. Wadhwa, and P. Rajan. Land use/land cover and land surface temperature analysis in wayanad district, india, using satellite imagery. *Annals of GIS*, 26(4):343–360, 2020.

[48] N. Kabisch, M. Strohbach, D. Haase, and J. Kronenberg. Urban green space availability in european cities. *Ecological indicators*, 70:586–596, 2016.

[49] H. Kim, S.-M. Choi, C.-S. Kim, and Y. J. Koh. Representative color transform for image enhancement. In *Proceedings of the IEEE/CVF international conference on computer vision*, pages 4459–4468, 2021.

[50] A. Kirillov, E. Mintun, N. Ravi, H. Mao, C. Rolland, L. Gustafson, T. Xiao, S. Whitehead, A. C. Berg, W.-Y. Lo, et al. Segment anything. In *Proceedings of the IEEE/CVF International Conference on Computer Vision*, pages 4015–4026, 2023.

[51] S. Kolhar and J. Jagtap. Convolutional neural network based encoder-decoder architectures for semantic segmentation of plants. *Ecological Informatics*, 64:101373, 2021.

[52] K. A. Korznikov, D. E. Kislov, J. Altman, J. Doležal, A. S. Vozmishcheva, and P. V. Krestov. Using u-net-like deep convolutional neural networks for precise tree recognition in very high resolution rgb (red, green, blue) satellite images. *Forests*, 12(1):66, 2021.

[53] S. Kulkarni, P. Deepa Shenoy, and K. Venugopal. Coffeegan: An effective data augmentation model for coffee plant diseases. In *International Conference on Data Management, Analytics & Innovation*, pages 431–443. Springer, 2023.

[54] A. C. K. Lee, H. C. Jordan, and J. Horsley. Value of urban green spaces in promoting healthy living and wellbeing: prospects for planning. *Risk management and healthcare policy*, pages 131–137, 2015.

[55] M. Y. Lilay and G. D. Taye. Semantic segmentation model for land cover classification from satellite images in gambella national park, ethiopia. *SN Applied Sciences*, 5(3):76, 2023.

[56] W. Liu, A. Yue, W. Shi, J. Ji, and R. Deng. An automatic extraction architecture of urban green space based on deeplabv3plus semantic segmentation model. In *2019 IEEE 4th International Conference on Image, Vision and Computing (ICIVC)*, pages 311–315. IEEE, 2019.

[57] M. Louhaichi, M. M. Borman, and D. E. Johnson. Spatially located platform and aerial photography for documentation of grazing impacts on wheat. *Geocarto International*, 16(1):65–70, 2001.

[58] G. E. Meyer and J. C. Neto. Verification of color vegetation indices for automated crop imaging applications. *Computers and electronics in agriculture*, 63(2):282–293, 2008.

[59] S. Minaee, Y. Boykov, F. Porikli, A. Plaza, N. Kehtarnavaz, and D. Terzopoulos. Image segmentation using deep learning: A survey. *IEEE transactions on pattern analysis and machine intelligence*, 44(7):3523–3542, 2021.

[60] M. V. Monteiro, K. J. Doick, P. Handley, and A. Peace. The impact of greenspace size on the extent of local nocturnal air temperature cooling in london. *Urban Forestry & Urban Greening*, 16:160–169, 2016.

[61] M. A. Moreno-Armendáriz, H. Calvo, C. A. Duchanoy, A. P. López-Juárez, I. A. Vargas-Monroy, and M. S. Suarez-Castañon. Deep green diagnostics: Urban green space analysis using deep learning and drone images. *Sensors*, 19(23):5287, 2019.

[62] T. Motohka, K. N. Nasahara, H. Oguma, and S. Tsuchida. Applicability of green-red vegetation index for remote sensing of vegetation phenology. *Remote Sensing*, 2(10):2369–2387, 2010.

[63] A. Mumuni and F. Mumuni. Data augmentation: A comprehensive survey of modern approaches. *Array*, 16:100258, 2022.

[64] C. Ng, T. Law, F. Jakarni, and S. Kulanthayan. Road infrastructure development and economic growth. In *IOP conference series: materials science and engineering*, volume 512, page 012045. IOP Publishing, 2019.

[65] A. Paszke, S. Gross, F. Massa, A. Lerer, J. Bradbury, G. Chanan, T. Killeen, Z. Lin, N. Gimelshein, L. Antiga, et al. Pytorch: An imperative style, high-performance deep learning library. *Advances in neural information processing systems*, 32, 2019.

[66] F. Perez, C. Vasconcelos, S. Avila, and E. Valle. Data augmentation for skin lesion analysis. In *OR 2.0 Context-Aware Operating Theaters, Computer Assisted Robotic Endoscopy, Clinical Image-Based Procedures, and Skin Image Analysis: First International Workshop, OR 2.0 2018, 5th International Workshop, CARE 2018, 7th International Workshop, CLIP 2018, Third International Workshop, ISIC 2018, Held in Conjunction with MICCAI 2018, Granada, Spain, September 16 and 20, 2018, Proceedings 5*, pages 303–311. Springer, 2018.

[67] S. Pervaiz, K. Javid, F. Z. Khan, B. Talib, R. Siddiqui, M. M. Ranjha, and M. A. N. Akram. Spatial analysis of vegetation cover in urban green space under new government agenda of clean and green pakistan to tackle climate change. *Journal of Ecological Engineering*, 20(4), 2019.

[68] I. Philipp and T. Rath. Improving plant discrimination in image processing by use of different colour space transformations. *Computers and electronics in agriculture*, 35(1):1–15, 2002.

[69] R. Popek, A. Przybysz, H. Gawrońska, K. Klamkowski, and S. W. Gawroński. Impact of particulate matter accumulation on the photosynthetic apparatus of roadside woody plants growing in the urban conditions. *Ecotoxicology and environmental safety*, 163:56–62, 2018.

[70] C. A. Queiroz and S. Gautam. *Road infrastructure and economic development: some diagnostic indicators*, volume 921. World Bank Publications, 1992.

[71] S. Qureshi, J. H. Breuste, and C. Y. Jim. Differential community and the perception of urban green spaces and their contents in the megacity of karachi, pakistan. *Urban Ecosystems*, 16:853–870, 2013.

[72] S. Qureshi, J. H. Breuste, and S. J. Lindley. Green space functionality along an urban gradient in karachi, pakistan: a socio-ecological study. *Human Ecology*, 38:283–294, 2010.

[73] N. Rizwan. *Urban greening: The potential and challenges of greening Karachi*. PhD thesis, Habib University, 2018.

[74] O. Ronneberger, P. Fischer, and T. Brox. U-net: Convolutional networks for biomedical image segmentation. In *Medical Image Computing and Computer-Assisted Intervention–MICCAI 2015: 18th International Conference, Munich, Germany, October 5-9, 2015, Proceedings, Part III 18*, pages 234–241. Springer, 2015.

[75] T.-Y. Ross and G. Dollár. Focal loss for dense object detection. In *proceedings of the IEEE conference on computer vision and pattern recognition*, pages 2980–2988, 2017.

[76] A. Russo and G. T. Cirella. Modern compact cities: how much greenery do we need? *International journal of environmental research and public health*, 15(10):2180, 2018.

[77] A. Saha, P. Prasad, and A. Thabit. Leveraging adaptive color augmentation in convolutional neural networks for deep skin lesion segmentation. In *2020 IEEE 17th International Symposium on Biomedical Imaging (ISBI)*, pages 2014–2017. IEEE, 2020.

[78] M. Saini and S. Susan. Tackling class imbalance in computer vision: a contemporary review. *Artificial Intelligence Review*, 56(Suppl 1):1279–1335, 2023.

[79] M. Sanderson, F. Taube, B. Tracy, M. Wachendorf, et al. Plant species diversity relationships in grasslands of the northeastern usa and northern germany. In *Multi-function grasslands: quality forages, animal products and landscapes. Proceedings of the 19th General Meeting of the European Grassland Federation, La Rochelle, France, 27-30 May 2002*, pages 842–843. Organizing Committee of the European Grassland Federation, 2002.

[80] Y. Shao and R. S. Lunetta. Comparison of support vector machine, neural network, and cart algorithms for the land-cover classification using limited training data points. *ISPRS Journal of Photogrammetry and Remote Sensing*, 70:78–87, 2012.

[81] A. Shoaib, K. Nadeem, H. S. Islam, and A. Saleemi. Assessing spatial distribution and residents satisfaction for urban green spaces in lahore city, pakistan. *GeoJournal*, pages 1–16, 2022.

[82] C. Shorten and T. M. Khoshgoftaar. A survey on image data augmentation for deep learning. *Journal of big data*, 6(1):1–48, 2019.

[83] K. K. Singh. Urban green space availability in bathinda city, india. *Environmental monitoring and assessment*, 190(11):671, 2018.

[84] M. W. Tarin, S. M. Nizami, R. Jundong, C. Lingyan, H. You, T. H. Farooq, M. Gilani, J. Ifthikar, M. Tayyab, and Y. Zheng. Range vegetation analysis of kherimurat scrub forest, pakistan. *International Journal of Development and Sustainability*, 6(10):1319–1333, 2017.

[85] A. Tariq, S. Siddiqui, A. Sharifi, and S. H. I. A. Shah. Impact of spatio-temporal land surface temperature on cropping pattern and land use and land cover changes using satellite imagery, hafizabad district, punjab, province of pakistan. *Arabian Journal of Geosciences*, 15(11):1045, 2022.

[86] C. J. Tucker. Red and photographic infrared linear combinations for monitoring vegetation. *Remote sensing of Environment*, 8(2):127–150, 1979.

[87] J. Ubbens, M. Cieslak, P. Prusinkiewicz, and I. Stavness. The use of plant models in deep learning: an application to leaf counting in rosette plants. *Plant methods*, 14:1–10, 2018.

[88] L. Velasquez-Camacho, M. Etxegarai, and S. de Miguel. Implementing deep learning algorithms for urban tree detection and geolocation with high-resolution aerial, satellite, and ground-level images. *Computers, Environment and Urban Systems*, 105:102025, 2023.

[89] F. Waldner and F. I. Diakogiannis. Deep learning on edge: Extracting field boundaries from satellite images with a convolutional neural network. *Remote sensing of environment*, 245:111741, 2020.

[90] Wan, Z., S. Hook, G. Hulley. Mod11a1 modis/terra land surface temperature/emissivity daily l3 global 1km sin grid v006 [data set]., 2015. NASA EOSDIS Land Processes Distributed Active Archive Center. https://doi.org/10.5067/MODIS/MOD11A1.006.

[91] J. Wang, Z. Zheng, A. Ma, X. Lu, and Y. Zhong. Loveda: A remote sensing land-cover dataset for domain adaptive semantic segmentation. In J. Vanschoren and S. Yeung, editors, *Proceedings of the Neural Information Processing Systems Track on Datasets and Benchmarks*, volume 1. Curran, 2021.

[92] D. Ward, P. Moghadam, and N. Hudson. Deep leaf segmentation using synthetic data. *arXiv preprint arXiv:1807.10931*, 2018.

[93] S. Waseem and U. Khayyam. Loss of vegetative cover and increased land surface temperature: A case study of islamabad, pakistan. *Journal of cleaner production*, 234:972–983, 2019.

[94] Wikipedia. List of world cities by population density. https://en.wikipedia.org/wiki/List_of_world_cities_by_population_density#cite_note-12, Accessed: 2023-06-03.

[95] L. Windrim and M. Bryson. Forest tree detection and segmentation using high resolution airborne lidar. In *2019 IEEE/RSJ International Conference on Intelligent Robots and Systems (IROS)*, pages 3898–3904. IEEE, 2019.

[96] H. Xu. Modification of normalised difference water index (ndwi) to enhance open water features in remotely sensed imagery. *International journal of remote sensing*, 27(14):3025–3033, 2006.

[97] M. Xu, S. Yoon, A. Fuentes, and D. S. Park. A comprehensive survey of image augmentation techniques for deep learning. *Pattern Recognition*, 137:109347, 2023.

[98] X. Yang and C. Lo. Using a time series of satellite imagery to detect land use and land cover changes in the atlanta, georgia metropolitan area. *International Journal of Remote Sensing*, 23(9):1775–1798, 2002.

[99] M. Yeung, E. Sala, C.-B. Schönlieb, and L. Rundo. Unified focal loss: Generalising dice and cross entropy-based losses to handle class imbalanced medical image segmentation. *Computerized Medical Imaging and Graphics*, 95:102026, 2022.

[100] G. Yin, A. Verger, I. Filella, A. Descals, and J. Peñuelas. Divergent estimates of forest photosynthetic phenology using structural and physiological vegetation indices. *Geophysical Research Letters*, 47(18):e2020GL089167, 2020.

[101] H. Yu, Y. Zhou, R. Wang, Z. Qian, L. D. Knibbs, B. Jalaludin, M. Schootman, S. E. McMillin, S. W. Howard, L.-Z. Lin, et al. Associations between trees and grass presence with childhood asthma prevalence using deep learning image segmentation and a novel green view index. *Environmental Pollution*, 286:117582, 2021.

[102] X. Yuan, J. Shi, and L. Gu. A review of deep learning methods for semantic segmentation of remote sensing imagery. *Expert Systems with Applications*, 169:114417, 2021.

[103] Y. Zeng, D. Hao, A. Huete, B. Dechant, J. Berry, J. M. Chen, J. Joiner, C. Frankenberg, B. Bond-Lamberty, Y. Ryu, et al. Optical vegetation indices for monitoring terrestrial ecosystems globally. *Nature Reviews Earth & Environment*, 3(7):477–493, 2022.

[104] Y. Zha, J. Gao, and S. Ni. Use of normalized difference built-up index in automatically mapping urban areas from tm imagery. *International journal of remote sensing*, 24(3):583–594, 2003.

[105] X. Zhang, Y. Zhou, and J. Luo. Deep learning for processing and analysis of remote sensing big data: A technical review. *Big Earth Data*, 6(4):527–560, 2022.

[106] Y. Zhang, P. David, and B. Gong. Curriculum domain adaptation for semantic segmentation of urban scenes. In *Proceedings of the IEEE international conference on computer vision*, pages 2020–2030, 2017.

[107] H. Zhao, J. Shi, X. Qi, X. Wang, and J. Jia. Pyramid scene parsing network. In *Proceedings of the IEEE conference on computer vision and pattern recognition*, pages 2881–2890, 2017.

[108] L. Zhou, C. Zhang, and M. Wu. D-linknet: Linknet with pretrained encoder and dilated convolution for high resolution satellite imagery road extraction. In *Proceedings of the IEEE conference on computer vision and pattern recognition workshops*, pages 182–186, 2018.

[109] T. Zhou, W. Wang, E. Konukoglu, and L. Van Gool. Rethinking semantic segmentation: A prototype view. In *Proceedings of the IEEE/CVF Conference on Computer Vision and Pattern Recognition*, pages 2582–2593, 2022.

[110] V. Žlender and C. W. Thompson. Accessibility and use of peri-urban green space for inner-city dwellers: A comparative study. *Landscape and urban planning*, 165:193–205, 2017.

[111] Y. Zou, Z. Yu, B. Kumar, and J. Wang. Unsupervised domain adaptation for semantic segmentation via class-balanced self-training. In *Proceedings of the European conference on computer vision (ECCV)*, pages 289–305, 2018.